3D RECONSTRUCTION OF INTERVERTEBRAL DISCS FROM T1-WEIGHTED MAGNETIC RESONANCE IMAGES

I. Castro[⋆‡], *L. Humbert*[‡⋆], *T. Whitmarsh*[⋆‡], *A. Lazary*[◇], *L.M. Del Río Barquero*[†] *and A.F. Frangi*[⋆‡±]

[⋆] Center for Computational Imaging & Simulation Technologies in Biomedicine (CISTIB), Universitat Pompeu Fabra, Barcelona, Spain

[‡]Biomedical Research Networking Center on Bioengineering, Biomaterials and Nanomedicine (CIBER-BBN), Barcelona, Spain.

[†]CETIR Centre Mèdic, Barcelona, Spain.

[◇] National Center for Spinal Disorders (NCSD), Budapest, Hungary.

[±] Department of Mechanical Engineering, University of Sheffield, Sheffield, UK

ABSTRACT

Low back pain is a current and increasing problem closely related to intervertebral disc degeneration, which is responsible for over 90% of spinal surgical procedures. In clinical routine, clinicians base their diagnosis of disc degeneration on 2D analysis of Magnetic Resonance (MR) images. In this work, an automatic 3D segmentation method, based on active shape models, is presented for both degenerated and normal intervertebral discs. A database of 25 intervertebral discs was used to semi-automatically build a shape statistical model and intensity models. Then, a 3D reconstruction was achieved by using those models to deform an initial shape. The method was evaluated using the 25 intervertebral discs and a leave-one-out cross validation, resulting in a mean shape accuracy of $1.6mm$ and a mean dice similarity index of 83.6%. This automatic and accurate 3D reconstruction method opens the way for an improved diagnosis of disc degeneration.

Index Terms— Statistical model, 3D, Intervertebral disc degeneration, image segmentation, MRI

1. INTRODUCTION

Low back pain is a well−known and widely spread musculoskeletal disorder. About 25% of the EU27 active population complain of low back pain [1]. With a prevalence estimates for chronic low back pain between 6 and 11% and an annual direct cost of 7000 euros per person [2].

Intervertebral discs are located between vertebrae in order to allow back movements and absorbing while distributing the loads applied to the spine. Disc degeneration is considered as one of the key factors of low back pain. In clinical routine, Magnetic Resonance (MR) is used to acquire images of the intervertebral discs. Clinicians observe sagittal images seeking for indications of degeneration and axial view to overcome doubts from unclear discs.

For the last ten years, new research lines have been focused on biomechanical models to improve understanding, diagnosis, or surgical treatments of disc degeneration [3], [4]. Such models require 3D meshes of the patient's discs, which are usually obtained by manual processing steps of the medical images [5].

As this process is highly time consuming, automatic methods to accurately reconstruct intervertebral discs are sought. In the literature most of the segmentation methods of the intervertebral discs are in 2D [6],[7], [8]. Seifert et al. [9] proposed a 3D reconstruction algorithm for intervertebral discs, but merging multiple 2D segmentations to obtain the 3D. In their paper, Schmidt et al. [10] used Markov chain to label every voxel in a 3D volume, in order to distinguish the different intervertebral discs. However, the method was not thought to perform a high accurate shape reconstruction.

A well-known method to obtain an accurate medical image segmentation is Active Shape Models (ASM) [11]. ASM is an iterative algorithm which seeks the best configuration of an object in an image, and it is based on a Point Distribution Model (PDM). A PDM is a statistical shape model, which restricts all the possible configurations the sought object can have. In each iteration of the ASM all the mesh points are displaced, searching for a better position inside the image. Then, the shape is updated to the closest one contained in the PDM.

An atlas-based 2D reconstruction method was proposed by Michopoulou [12], in which ASM was used to segment the discs and a post-procesing step, based on fuzzy logic [13], was used to improve the accuracy. However, the method was limited to the analysis of 2D MR slices.

This paper presents an automatic 3D reconstruction and mesh creation method of intervertebral discs. The method is

The research leading to these results has received funding from the European Union Seventh Framework Programme (FP7/2007-2013) under grant agreement number 269909, MySpine project. The work of Alejandro Frangi is partially funded by the ICREA-Academia programme. The work of Tristan Whitmarsh is supported by the sub-programme PFIS (Ayudas predoctorales de formación en investigación en salud), an initiative funded by Acción Estratégica de Salud in the National R&D&i Plan 2008-2011 and financed by the Instituto de Salud Carlos III. The research leading to these results has been partially funded by the Spanish Ministry Science and Innovation (ref. TIN2009-14536-C02-01), Plan E and ERDF funds.

based on ASM, which was trained with 3D images created by interpolation of sagittal T1-weighted MR images. The method starts by manually positioning the initial shape in the center of the disc to be reconstructed. Then, the statistical model is applied to deform this initial shape until an accurate reconstruction is obtained. A leave-one-out cross validation of the method is proposed by using a database of 25 MR images.

2. METHOD

The reconstruction method proposed in this paper is mainly based on ASM principles developed by Cootes et al. [11]. ASM are also known as smart snakes, whose internal energy is given in the form of a PDM, and the external energy is obtained from the intensity profiles along the normals of the points in the PDM. In this paper, the PDM was created following a similar pipeline to the one proposed by Frangi et al. [14]. The external energy follows the original idea of Cootes et al.

2.1. Data

A database of T1-weighted MR images of 25 human L3-L4 intervertebral discs, using an open MR machine of 0.4 Tesla (Hitachi, Twinsburg, Ohio) was collected at the National Center for Spinal Disorders (Budapest, Hungary). Patients were 13 males and 12 females with a mean age of 44 (age interval: 27-62 years). Those patients were selected for participating in the European MySpine project. The study design received approval of the institutional review board and written informed consent was retrieved from all subjects.

All the images were resampled from an initial size of 0.68x0.68x4.0 mm^3 to a final size of 0.68x0.68x0.68 mm^3.

Using the classification of Pfirrmann [15] for intervertebral disc degeneration (grades I to V), there were 2 discs with a degeneration of grade I (healthy), 10 with a grade II, 9 with a grade III and 4 with a grade IV.

2.2. Statistical model construction

The first step pursued to construct the PDM was to manually segment the L3-L4 intervertebral discs of the patients involved in this study. ITK-SNAP [16] was used to identify the region of interest of the intervertebral discs, from which binary masks were computed and then transformed to distance maps. One of those masks was selected as the reference one. It was smoothed using morphological operations and its surface mesh and distance map were created.

Then, a surface mesh from every disc was computed following the pipeline depicted in Fig. 1.

First of all, the set of distance maps was aligned to the reference one using a registration method based on similarity transform and a mean square metric [14]. Then, a non-rigid registration algorithm, based on B-splines, was applied on the reference distance map to deform it to all the previously aligned distance maps. These non-rigid transformations were applied to the reference mesh to automatically achieve all the shapes corresponding to the manually segmented discs.

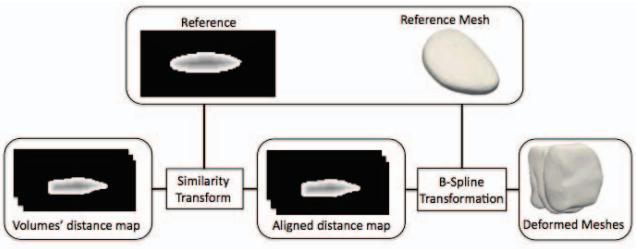


Fig. 1: Alignment and surface mesh creation pipeline

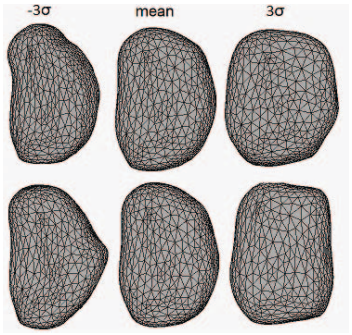


Fig. 2: First two modes of variation of the PDM (± 3 standard deviation (σ) from the mean)

Having all the shapes aligned, the PDM was computed as follow. A $3n \times M$ matrix (D) was created, where n was the number of points in the mesh and M the number of shapes. Every row of the matrix contained the points' coordinates of the i^{th} shape minus the points' coordinates of the mean shape, $row_i = [|x_{i1} - \bar{x_1}|, |y_{i1} - \bar{y_1}|, |z_{i1} - \bar{z_1}|...|x_{in} - \bar{x_n}|, |y_{in} - \bar{y_n}|, |z_{i1} - \bar{z_n}|]$. Principal Component Analysis (PCA) [11] was then applied to D. PCA computes an orthonormal basis whose axis are aligned with the statistical variations in the data. Those axis are the eigenvectors of the covariance of D and their importance is measured by their eigenvalues. New shape instances s_{new} can be obtained using equation 1:

$$s_{new} = \bar{s} + Q \cdot a \tag{1}$$

where $\bar{s}$ is the mean shape and a is a vector containing the weight of every eigenvector and Q the matrix of ordered eigenvectors. The first two modes of variation of the statistical model, created with the 25 patients included in this study, are shown in Fig. 2.

This previous PDM, represents the internal energy of the snake. The external energy was stored in the form of an intensity model. In Fig. 3, the pipeline to compute the intensity model is depicted in 2D to simplify. However, the actual method is in 3D.

First of all, the similarity transformations, previously computed to aligned the distance maps, were applied to the

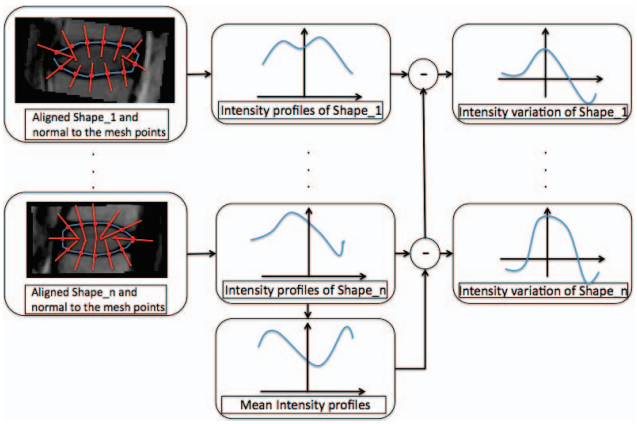


Fig. 3: **Illustration in 2D of the extraction of the intensity profiles. Although only one intensity profile per disc is shown, intensity profiles were computed at each point of the surface mesh.**

original MR images. From this aligned MR images, intensity profiles along the normal of the points of their corresponding meshes were extracted. The average profiles were computed and subtracted from the original ones, which, together with the mean intensity, represented the intensity model.

All the methods were implemented in C++ and taking advantage of ITK library [17].

2.3. Reconstruction Method

The reconstruction method required the manual identification of the center of the disc in the MR images in order to initialize the mean instance of the statistical model. Then, an iterative process started, in which all the points of the mesh were displaced along their normal directions, using the intensity model, to achieve a new shape. This displacement was obtained by seeking the minimum mahalanobis distance [11] between the intensity profiles, in the targeted image, and the mean intensity given by the intensity model.

This new shape and Q were used as input of equation 1 to compute a. Q and a were used in equation 1 again to obtain the final shape for this iteration. The process finished when the a did not change more than a threshold.

2.4. Evaluation of the method

Due to the small number of lumbar discs available, a leave-one-out cross validation was performed. 25 different statistical models were created with 24 different discs, leaving one different disc out in every model.

In order to evaluate the accuracy of the method, point-to-surface distances and Dice Similarity Index (DSI) [18] between the reconstructed shape and ground truth (shape extracted from the manual segmentations performed using ITK-SNAP) were computed.

DSI is defined in equation 2, where GT represents the Ground Truth and RD the Reconstructed Disc.

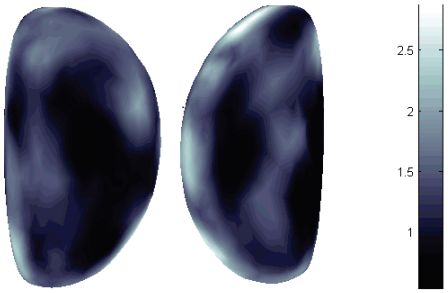


Fig. 4: **Average distance, from the reconstruction to the ground truth, of all the reconstructions in every voxel.**

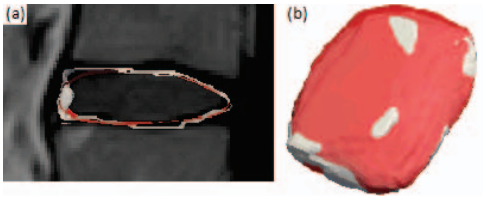


Fig. 5: **(a) Sagittal MR slice of a patient with the contour of the reconstructed surface mesh (red) and the contour of the ground truth (white). (b) 3D superimposition of the reconstructed surface mesh (red) and the ground truth surface mesh (white)**

$$DSI = \frac{2 \times (GT \cap RD)}{GT + RD} \times 100\% \quad (2)$$

A perfect reconstruction would reach a DSI of 100%.

3. RESULTS

The evaluation of the method resulted in mean point-to-surface distance between the reconstructed meshes and ground truth of 1.6mm, with a 2 Root Mean Square distance of 3.5mm (statistically meaning that 95% of the distances were below this threshold). In Fig. 4, a map of the average point-to-surface distances is presented. Regarding the DSI, A mean ($\pm$ 2 standard deviation) of $83.6 \pm 9.6\%$ was found (Fig. 5).

Fig. 5 shows a 2D MR slice of one patient with the contour of the reconstructed shape and the one of the ground truth. On the right the 3D superimposition of the reconstructed and ground truth surface meshes. The DSI of this patient's disc was 81.1 % and the mean point-to-surface distance was 1.2mm.

4. DISCUSSION

This study aimed at proposing a method to obtain a 3D reconstruction of intervertebral discs from MR images.

With a mean shape accuracy of 1.6mm, the method was found to be quite accurate, taking into consideration that the spacing between two consecutive sagittal MR slices was 4mm, which provided to the reconstruction method with few

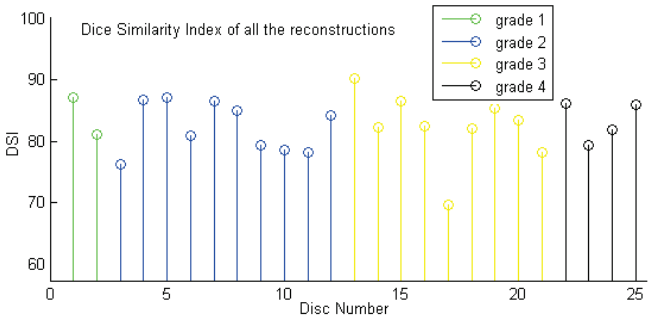


Fig. 6: **DSI from all of the reconstructed discs.**

information in the perpendicular direction to the slices, when deforming the initial mesh using the statistical model.

The minimum DSI was 68.9%, obtained from patient 12 (Fig. 6), which appears to be a clear outlier among the evaluated discs. In fact, this disc presented a particular shape and none of other discs, in the set of intervertebral discs, had a shape similar to this one. Hence, the PDM could not perform a good approximation of the real disc. This limitation is due to the relatively low number of samples including in this study. Therefore, one of our future tasks is to include more patients to develop and validate the method (as well as more intervertebral disc levels), which will result in an improved generalization ability of the statistical model, allowing it to reconstruct such particular discs.

The last limitation is the need of user interaction for initializing the primary shape. This step could be automatized by detecting the center of the intervertebral disc in the center sagittal slice using image processing methods to detect the intervertebral discs [6] or [9].

5. CONCLUSIONS

This paper presents an automatic and accurate method to reconstruct intervertebral discs in 3D from MR using ASM. The next step will be to overcome the encountered limitations by including more samples in the study, and by using additional MR slices views (coronal or axial) together with the sagittal one to improve the 3D resolution of the volumes.

This method opens the way to a better diagnosis of disc degeneration, using advanced modeling and prediction methods such as biomechanical models.

6. REFERENCES

[1] European Agency for Safety and Health at Work: Zinta Podniece, "Work-related musculoskeletal disorders: prevention report," 2008.

[2] Junipert M., Kim Le T., and Mladsi D., "The epidemiology, economic burden, and pharmacological treatment of chronic low back pain in france, germany, italy, spain and the uk: a literature based review," *Expert Opin. Pharmacother*, vol. 10, pp. 2581–2592, 2009.

[3] Campana S., Charpail E., De Guise J.A., Rillardon L., Skalli W., and Mitton D., "Relationships between viscoelastic properties of lumbar intervertebral disc and degeneration grade assessed by MRI," *Journal of the Mechanical Behavior of Biomedical Materials*, vol. 4, no. 4, pp. 593 – 599, 2011.

[4] Galbusera F., Schmidt H., Noailly J., Malandrino A., Lacroix D., Wilke H., and Shirazi-Adl A., "Comparison of four methods to simulate swelling in poroelastic finite element models of intervertebral discs," *Journal of the Mechanical Behavior of Biomedical Materials*, vol. 4, no. 7, pp. 1234 – 1241, April 2011.

[5] Li H. and Wang Zh., "Intervertebral disc biomechanical analysis using the finite element modeling based on medical images," *Computerized Medical Imaging and Graphics*, vol. 30, no. 6-7, pp. 363 – 370, 2006, Medical Imaging and Telemedicine.

[6] Ruiqiong Sh., Dongmei S., Zhengding Q., and Weiss K.L., "An efficient method for segmentation of MRI spine images," in *Complex Medical Engineering, 2007. CME 2007. IEEE/ICME International Conference on*, may 2007, pp. 713 –717.

[7] Peng Zh., Zhong J., Wee W., and Lee Jing-huei, "Automated vertebra detection and segmentation from the whole spine MR images," in *Engineering in Medicine and Biology Society, 2005. IEEE-EMBS 2005. 27th Annual International Conference of the*, jan 2005, pp. 2527 –2530.

[8] Chevrefils C., Chériet Ch., Grimard G., and Aubin C.E., "Watershed segmentation of intervertebral disk and spinal canal from MRI images," in *4th International Conference on Image Analysis and Recognition (ICIAR 2007)*. 2007, p. 10171027, Springer-Verlag Berlin Heidelberg.

[9] Seifert S., Wachter I., Schmelzle G., and Dillmann R., "A knowledge-based approach to soft tissue reconstruction of the cervical spine," *Medical Imaging, IEEE Transactions on*, vol. 28, no. 4, pp. 494 –507, april 2009.

[10] Schmidt S., Bergtholdt M., Dries S., and Schnrr Ch., "Spine detection and labeling using a parts-based graphical model," in *20th International Conference on Information Processing in Medical Imaging (IPMI 2007)*, 2007, pp. 122–133.

[11] Cootes T.F., Taylor C.J., and Graham J., "Active shape models- their training and applications," *Computer Vision and image understanding*, vol. 61, no. 1, pp. 38–59, 1995.

[12] Michopoulou S.K., Costaridou L., Panagiotopoulos E. Speller R., Panayiotakis G., and Todd-Pokropek A., "Atlas-based segmentation of degenerated lumbar intervertebral discs from MR images of the spine," *Biomedical Engineering, IEEE Transactions on*, vol. 56, no. 9, pp. 2225 –2231, sept. 2009.

[13] Young Sik Choi and Krishnapuram R., "A robust approach to image enhancement based on fuzzy logic," *Image Processing, IEEE Transactions on*, vol. 6, no. 6, pp. 808 –825, jun 1997.

[14] Frangi A.F., Rueckert D., Schnabel J.A., and Niessen W.J., "Automatic construction of multiple-object three-dimensional statistical shape models: application to cardiac modeling," *Medical Imaging, IEEE Transactions on*, vol. 21, no. 9, pp. 1151 –1166, sept. 2002.

[15] Pfirrmann Ch. W. A., Metzdorf A., Zanetti M., Hodler J., and Boos N., "Magnetic resonance classification of lumbar intervertebral disc degeneration," in *Spine*, 2001, vol. 26, pp. 1873–1878.

[16] Yushkevich P. A., Piven J., Hazlett H. C., Smith R. G., Ho S., Gee J. C., and Gerig G., "User-guided 3D active contour segmentation of anatomical structures: significantly improved efficiency and reliability.," *NeuroImage*, vol. 31, pp. 1116–28, 2006 Jul 1 2006.

[17] Ibánez L., Schroeder W., Ng L., and J. Cates, *The ITK Software Guide*, Kitware, Inc. ISBN 1-930934-15-7, http://www.itk.org/ItkSoftwareGuide.pdf, second edition, 2005.

[18] Zijdenbos A. P., Dawant B. M., Margolin R. A., and Palmer A. C., "Morphometric analysis of white matter lesions in MR images: method and validation," *Medical Imaging, IEEE Transactions on*, vol. 13, no. 4, pp. 716–724, 1994.